

Special Issue

CICE 2018 - FRP composites in construction: Advances in material research & engineering

Effect of hygrothermal environment on traction-separation behavior of carbon fiber/epoxy interface



Lik-ho Tam^a, Ao Zhou^b, Runxiao Zhang^c, Chao Wu^{a,*}

^aSchool of Transportation Science and Engineering, Beihang University, 37 Xueyuan Road, Beijing 100191, China

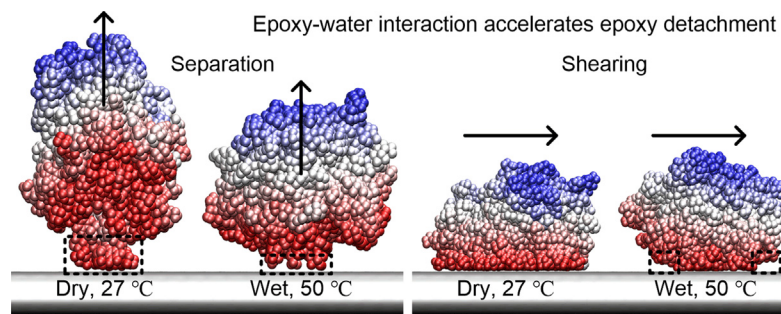
^bSchool of Civil and Environmental Engineering, Harbin Institute of Technology, Shenzhen, Shenzhen 518055, China

^cDepartment of Civil and Mineral Engineering, University of Toronto, Toronto, Ontario M5S 1A4, Canada

HIGHLIGHTS

- Epoxy-water interaction accelerates the detachment of epoxy molecule.
- The accumulated water molecules reduce interfacial adhesion and shear resistance.
- Interfacial mechanical properties degrade severely in hygrothermal environment.
- Interfacial traction-separation responses of the cohesive zone model are investigated.

GRAPHICAL ABSTRACT



ARTICLE INFO

Article history:

Received 14 March 2019

Received in revised form 23 May 2019

Accepted 10 June 2019

Available online 24 June 2019

Keywords:

Interface

Traction-separation

Hygrothermal environment

Molecular dynamics simulation

ABSTRACT

The strong interfacial interaction between carbon fiber and epoxy matrix plays a key role in ensuring the performance of carbon fiber reinforced polymer (CFRP). During a prolonged service-life, CFRP is inevitably exposed to the hygrothermal environment and the integrity of fiber/matrix interface is most vulnerable, but the microscopic behavior of the interface under the environmental exposure remains elusive. Here an atomistic analysis is presented on mode I and mode II traction-separation behavior between carbon fiber and epoxy matrix, which provides insights into how the surrounding water molecules at different temperature levels impact the interfacial behavior. It is found that the water molecules at the interface reduce the contact area between fiber and matrix and weaken the epoxy properties by disrupting the molecular interactions, which consequently lowers the energy barriers to interfacial separation and sliding, and the elevated temperature level further degrades the interfacial mechanical response as the epoxy becomes softened. The research findings demonstrate that the presence of water drastically deteriorates the integrity of carbon fiber/epoxy interface, and the derivation of cohesive laws based on traction-separation simulation results provides a paradigm of deriving the fundamental inputs for a multiscale modeling of the interface at the continuum level by considering the environmental effect.

© 2019 Elsevier Ltd. All rights reserved.

1. Introduction

Carbon fiber reinforced polymer (CFRP) is a type of remarkably resilient composite material possessing outstanding properties, such as high specific stiffness- and strength-to-weight ratios, good

* Corresponding author.

E-mail address: wuchao@buaa.edu.cn (C. Wu).

thermal stability, and strong corrosion resistance. CFRP composite has emerged as a viable alternative to the conventional materials in construction industry, such as applications in concrete infrastructures as external confinement/reinforcement and internal rebar [1–3]. Despite the promise as reinforcement of existing infrastructures and structural building-block in new constructions, CFRP composite exhibits a certain degree of property degradation under the environmental exposure, which shortens the intended service-life [4–9]. These problems are usually attributed to the deterioration of interfacial integrity between carbon fiber and epoxy matrix, which is crucial to the performance of these macroscale applications involving CFRP composite [9,10]. In the hygrothermal environment, the epoxy functional groups and molecular-size structural voids in the bonded interface facilitate the absorption of water, which severely affects the structure and properties of CFRP composite [11,12]. For the exposed CFRP composite, the fiber/matrix interface is particularly vulnerable under the external load, as evidenced by the relatively clean fiber surface after failure [13,14]. From these previous studies, it is inferred that the interface between carbon fiber and epoxy matrix mainly governs the long-term properties of CFRP composite, which should be better understood to ensure the durability.

Extensive efforts have been made to explore what happens to the fiber/matrix interface in the presence of water as a result of moisture absorption, as shown in Fig. 1(a) and (b), with the focus on the situations between water and interfaces at the microscale [9,10,14–18]. In particular, the interfacial fracture energy of single carbon-fiber epoxy composite can decrease by 50% after seven-day immersion in 70 °C water [14]. The interfacial deterioration after the wet environmental exposure or the water immersion is related to the structural changes of interfacial region, where the width of the exposed interfacial region increases and the interfacial debonding occurs, even without the external load [15–17]. It is noted that these earlier experimental studies are mainly conducted in characterizing the structural and property variations affected by the environmental exposure, which lack sufficient physical understandings on how the stress transfer at the interface is disrupted or altered by the presence of water. Meanwhile, it is difficult to obtain the stress transfer information of the local interface between fiber and matrix under the environmental exposure experimentally, due to the lack of appropriate spatiotemporal resolution.

In order to understand the situation in interfacial region between fiber and matrix, numerical simulation using the continuum modeling has been used, as it considers the constituent interactions and the variations of material and structure that occur at the smaller length scale, and hence the interfacial failure process can be properly simulated. The numerical simulation based on finite element analysis of the FRP composite generally incorporates a cohesive zone model to represent the interfacial region between fiber and matrix, as shown in Fig. 1(c). In cohesive zone model, the

fracture process is governed by the traction-separation law, which describes the relationship between cohesive traction and separation displacement at the crack tip during the interfacial failure process. The cohesive zone modeling method has been adopted in recent simulations of carbon fiber/epoxy composites, which allows for the prediction of interfacial debonding and composite property degradation in different environmental conditions of temperature and humidity [19–24]. Although the interfacial laws are used in these computational studies to account for the interaction between fiber and matrix, the applied laws are mainly derived from the macroscale experimental test or the parametric studies, which are not able to reflect the physics behind the interfacial damage initiation and evolution existed at a smaller level. Therefore, the detailed structural configuration of the bonded materials and the actual interactions at the microscale are still not clear.

As the local fiber/matrix interface and water molecules possess comparable nanoscale dimensions, atomistic molecular dynamics (MD) simulations are considered as a powerful tool for characterizing the load transfer behavior at the interface, especially in consideration of the environmental exposure. In previous MD simulation studies, several parallel graphene sheets are used to represent the graphite crystallite of carbon fiber outer-layer without the sizing, as shown in Fig. 1(d) [25–27]. For epoxy matrix, a computational strategy is adopted for cross-linking the epoxy molecule, which is placed on top of the graphene sheets to form the molecular model of fiber/matrix interface. The molecular interface formation between fiber and matrix is investigated previously, where the width of interfacial region estimated from MD simulation agrees with the transmission electron microscopy observation of a carbon/epoxy composite [26]. In the investigation of the environmental effect, the interface model is generally immersed in water or saltwater to simulate the saturated state of moisture absorption in the local interfacial region, and hence the maximum impact on the interfacial properties is explored [27–29]. It is challenging to simulate the chemical reaction of such system involving few tens of thousands of water molecules using the reactive force field [30,31], as excessive computational power is required. Comparatively, the empirical force field is used to simulate the interactions between interface and surrounding solution. The interfacial adhesion is found to decrease by over 70% when the interface is fully immersed in water or saltwater [27–29], which is in good accord with the loss of mechanical and interfacial properties of the exposed CFRP composite at the macroscopic level [9,10,13–18,27,32]. By examining the simulation process, it is observed that the presence of water molecules in the bonded interface is one of the major reasons for the adhesion decrease. Although these studies have provided meaningful information about the interactions between interface and surrounding solution at the molecular level, the microscopic detail of traction-separation behavior of the interface in the hygrother-

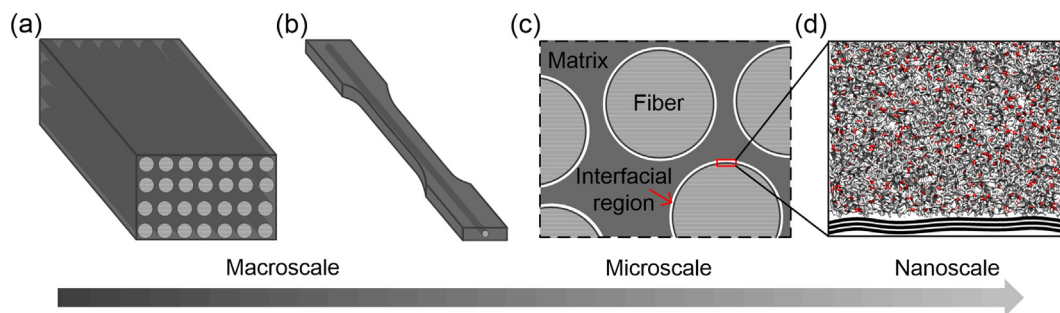


Fig. 1. Multiscale investigation of carbon fiber reinforced polymer (CFRP) composite: the (a) composite component and (b) single-fiber composite used in the macroscale experiment; (c) the microscale finite element analysis consisting of fiber/matrix interfacial region represented by the cohesive zone model; and (d) the nanoscale interface model consisting of epoxy molecule bonded to fiber surface used in the molecular dynamics (MD) simulation.

mal environment is still unknown, which limits the understanding of the load transfer at the fiber/matrix interface under the environmental exposure. Moreover, the interfacial properties, which are required to investigate the environmental effect on the interface within a multiscale analysis, are not provided in previous studies.

In this paper, we aim to understand the molecular interactions between carbon fiber and epoxy matrix, where the effects of the hygrothermal environment on mode I and mode II traction-separation behavior of the interface are investigated by MD simulation. The cross-linked epoxy molecule is bonded to the planar substrate representing the nanoscale fiber outer-surface to form the molecular interface model, which is conditioned in the dry and wet environments at room and elevated temperatures to simulate various environmental conditions. Interfacial separation studies in normal and shearing directions are simulated to assess the effect of the environmental exposure on the load transfer characteristics of the bonded interface in terms of force-separation responses, which are used to formulate the cohesive zone law for the fiber/matrix interface. The development of atomistically informed cohesive law illustrates how to derive the fundamental inputs for a continuum micromechanics model to study the effect of the hygrothermal environment on the overall response of composite at the microscale. The molecular simulation of the interfacial traction-separation behavior provides a valuable tool in identifying the microscopic situation of the interfacial damage in FRP composites under various environmental exposures.

2. Computational method

2.1. Force field and molecular model

In the simulation of the molecular interface model, the consistent valence force field (CVFF) is used, which includes bond, angle, dihedral, improper, and non-bonded terms (both van der Waals (vdW) and electrostatic interactions), with the form of the potential energy expression shown in the Supplementary Material in a previous study [33]. Particularly, the vdW and short-range electrostatic interactions are cutoff at 1.0 nm, as the interaction between non-bonded atoms beyond this distance is quite small, while the long-range electrostatic interaction is treated by the particle-particle mesh solver [34]. For the partial charge of atoms, it is determined by using the bond increment method, as defined in CVFF potential [35]. The parameters and partial charges from CVFF potential have been successfully used in the simulation of epoxy-bonded systems [27–29,36–38]. For the water molecules, the parameters of TIP3P water model are used [39]. The full set of parameters used to simulate the interface model is provided in previous studies [28,33]. The equilibration and deformation of

the interface are performed using the open source code LAMMPS with a time step of 1 fs [40].

To investigate how the environmental exposure affects the traction-separation behavior of the fiber/matrix interface, the molecular model consisting of epoxy molecule bonded to the substrate representing the nanoscale fiber surface is generated [28]. The epoxy molecule possesses the cross-linked network originated from the monomer formed by bisphenol A diglycidyl ether (DGEBA), with the dimensions of 5.9 nm × 5.9 nm × 4.7 nm, as shown in Fig. 2(a). The detailed cross-linking process is introduced in previous studies [29,33,36]. The molecular model of carbon fiber outer-layer is generally represented by several parallel graphene sheets in previous simulation studies, which interact with the resin mainly through vdW interaction, as electrostatic interactions between zero-charged carbon atoms in graphene sheets and resin molecule are small [25–27,41,42]. In this work, the configuration of the inert and impenetrable graphene sheets is simulated using a planar energetic wall, which is normally used as the substrate in various polymer-bonded systems [28,29,37,38]. The details of the molecular interface model used in this study are provided in the Appendix A. As this study focuses on the effect of the environmental exposure on the traction-separation behavior, the interface models without and with water molecules are studied, which are referred to as dry and wet interfaces, respectively. To create the dry interface, the epoxy molecule is placed on top of the planar wall at 0.5 nm. Periodic boundary conditions are applied in the interfacial plane, with the non-periodic boundary condition normal to the interface. The interface model is equilibrated at a temperature of 300 K for 2 ns in the canonical (NVT) ensemble to reach the equilibrium state, with the Nosé–Hoover thermostat for the temperature control [43]. For the wet interface, a water layer surrounding the equilibrated model is added with a density of 1.0 g·cm⁻³, which corresponds to the moisture saturated state, as shown in Fig. 2(b). In the applied boundary condition, water molecules can move across the simulation cell boundary to mimic the infinitely large water layer. To simulate the hygrothermal environment, the investigated temperature levels are set as 27 and 50 °C, denoting the temperature range that the civil infrastructure commonly suffers during the service-life [44].

2.2. Simulation of traction-separation behavior

After the dry and wet interfaces are constructed, the systems are equilibrated for 1 ns in the NVT ensemble in the simulated conditions. Specifically, the atoms in the epoxy molecule as well as the water molecules in the case of wet interface are free to move and contact with the planar wall to reach the equilibrium state. This equilibrium state is indicated by examining the mean squared

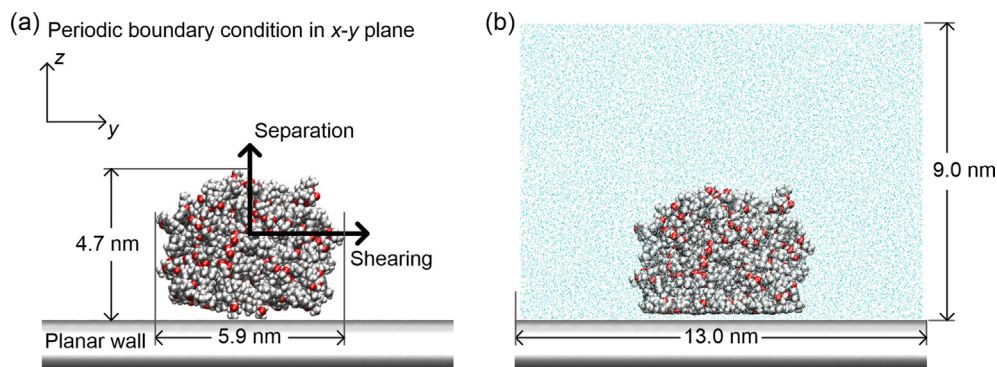


Fig. 2. The molecular interface model in the (a) dry and (b) wet environment, which consists of epoxy molecule bonded to the planar energetic wall representing the carbon fiber surface: the pulling directions corresponding to the normal separation and shearing of the interface are indicated.

displacement (MSD) of epoxy atoms during the equilibration process, which is calculated as

$$\text{MSD} = \frac{1}{N} \sum_{i=1}^N \left(|r_i(t) - r_i(t_0)|^2 \right), \quad (1)$$

where N is the number of epoxy atoms, $r_i(t)$ is the atomic coordinates at time t , and t_0 is the starting time of the equilibration process. For the different interfaces, the MSD of epoxy atoms recorded during the 1 ns NVT equilibration is shown in Fig. 3(a), which oscillates constantly before the equilibration is completed. Together with the constant oscillation of center of mass, temperature, and potential energy of epoxy molecule as shown in Fig. 3(b)–(d), it demonstrates that the equilibrium state of the simulated systems is achieved before the interfacial separation simulation. To verify the simulated water, the self-diffusion coefficient D of water molecules at the two investigated temperature levels are compared to the experimental measurement, which is calculated according to the Einstein relation [45], and it is proportional to the MSD versus a given time:

$$D = \frac{1}{6N} \lim_{t \rightarrow \infty} \frac{d}{dt} \sum_{i=1}^N \left(|r_i(t) - r_i(t_0)|^2 \right) = \frac{\Delta \text{MSD}}{6\Delta t}. \quad (2)$$

The MSD of water molecules recorded during the 1 ns NVT equilibration is shown in Fig. 3(e), for the two investigated temperature levels. The occasional drop of water MSD is because that when the upper-surface water molecules leave the water layer, they are considered as the single molecules and removed from the water layer, and hence the MSD measurement from a smaller amount of water molecules decreases. By performing linear regression of the recorded MSD, the self-diffusion coefficient D of water molecules is calculated as 2.44×10^{-9} and $3.70 \times 10^{-9} \text{ m}^2 \cdot \text{s}^{-1}$ for the investigated temperature levels of 27 and 50 °C respectively, which are close to the experimental measurements of 2.24×10^{-9} and $3.47 \times 10^{-9} \text{ m}^2 \cdot \text{s}^{-1}$ at the temperature levels of 25 and 45 °C [46]. Meanwhile, the temperature of water molecules also oscillates at the simulated temperature levels as shown in Fig. 3(f), which demonstrates that the water molecules are properly simulated. Apart from these quantities, the non-bonded interaction energy between epoxy and water and that between epoxy atoms

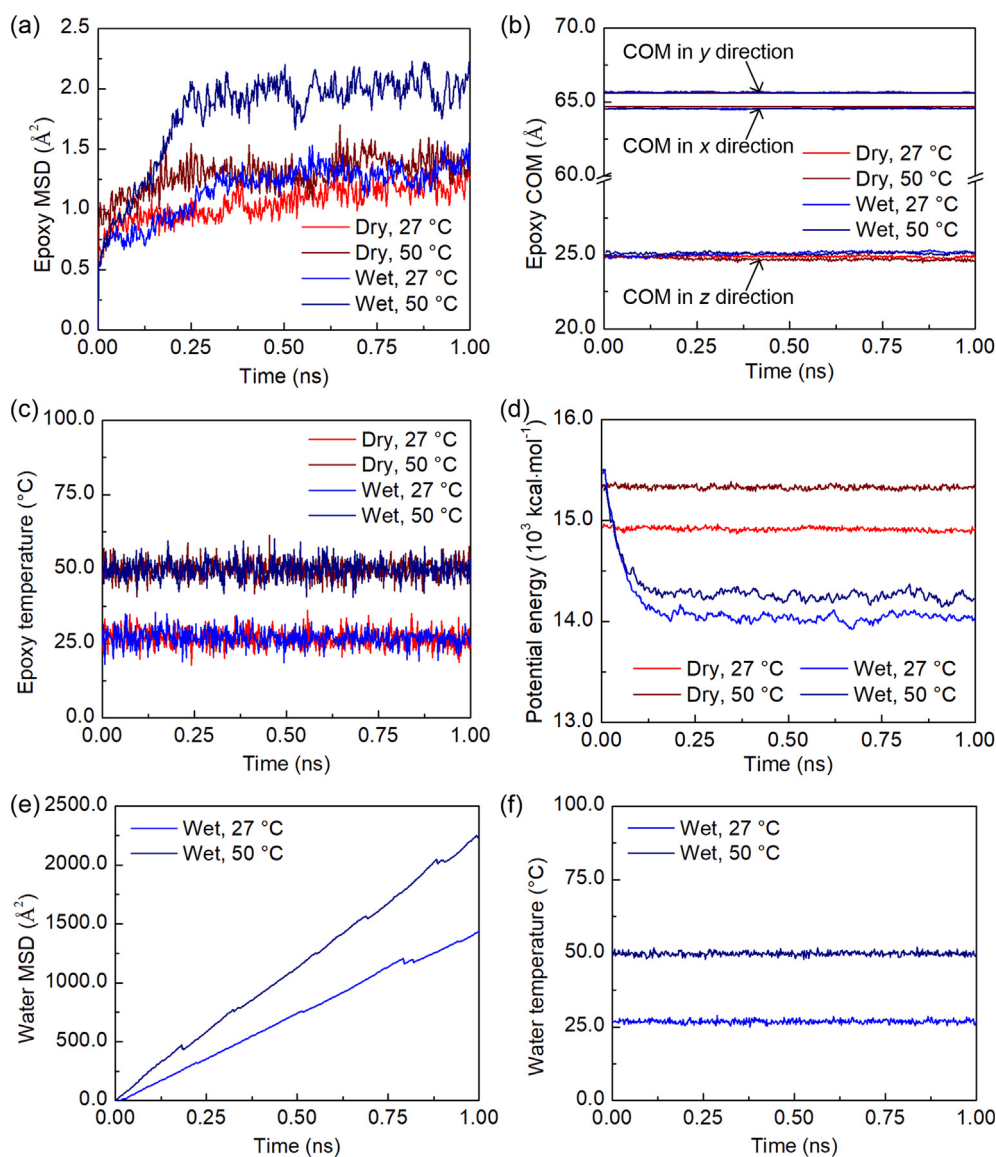


Fig. 3. The (a) mean squared displacement (MSD), (b) center of mass (COM), (c) temperature, and (d) potential energy of epoxy molecule recorded during the equilibration process: the constant oscillation of these quantities demonstrates that the interfaces have reached the equilibrium state; and the (e) MSD and (f) temperature of water molecules.

are recorded at every 2 ps and the interface configuration is saved at every 10 ps during the equilibration process, so as to further understand the conditions at the fiber/matrix interface under various environmental exposures.

To determine the interfacial traction-separation behavior under different environmental exposures, the interfacial failure process is simulated using steered molecular dynamics (SMD) simulation, where an external force is applied to the epoxy atoms to effectively mimic the atomic force microscopy experiment. In SMD simulation, the mass center of epoxy molecule is subject to the pulling force to simulate the interfacial separation and shearing, as indicated in Fig. 2(a). A constant pulling rate of $2.5 \text{ m}\cdot\text{s}^{-1}$ and a spring constant of $200.0 \text{ kcal}\cdot\text{mol}^{-1}\cdot\text{\AA}^{-2}$ are employed to allow for adequate response of epoxy atoms under pulling and to reduce the oscillation of the pulled epoxy atoms. The chosen parameters are consistent with previous studies and are appropriate to avoid any issues associated with the dependence of the pulling rate [28,37,38]. In addition, a brief discussion about the dependence of pulling rate on the interfacial behavior is included in the Appendix B. In each investigated condition, three independent starting configurations of the interface taken every 100 ps apart after the structural equilibration are studied by the SMD simulations to calculate the average interfacial work and to accurately determine the interfacial behavior associated with the different failure modes.

3. Results and discussion

3.1. Conditions of fiber/matrix interface in hygrothermal environment

In order to understand the effect of the hygrothermal environment, the conditions at the fiber/matrix interface affected by the surrounding environment are characterized. In wet condition, the water molecules affect the interaction between epoxy molecule and the bonded planar wall, as well as forming strong interaction with epoxy molecules, with the interaction energy of $-1554.6 \pm 23.5 \text{ kcal}\cdot\text{mol}^{-1}$ at $27 \text{ }^\circ\text{C}$. Due to the favorable epoxy-water interaction, the epoxy molecule is subject to great interfacial tension, which results in the decreased contact area with the bonded substrate, changing from $27.4 \pm 0.3 \text{ nm}^2$ in dry condition to $26.8 \pm 0.1 \text{ nm}^2$ in wet condition for the $27 \text{ }^\circ\text{C}$ cases, and similar contact area reduction is observed for the $50 \text{ }^\circ\text{C}$ cases. In recent simulation studies of epoxy-silica and epoxy-cellulose interfaces, such contact area reduction in wet condition is also reported [36,47]. It is noted that the reported value is the time-averaged number from the last 30 ps equilibration trajectory. As the configuration of epoxy molecule varies in different conditions, the cohesive energy of epoxy changes correspondingly. Specifically, cohesive energy is related to the energy required to eliminate all intermolecular forces of epoxy molecule, which is associated with the non-bonded interactions between epoxy atoms, including vdW and electrostatic interactions. In dry condition at $27 \text{ }^\circ\text{C}$, the non-bonded interaction energy is calculated to be $3772.0 \pm 6.9 \text{ kcal}\cdot\text{mol}^{-1}$, which decreases to $3048.2 \pm 9.7 \text{ kcal}\cdot\text{mol}^{-1}$ when water is presented, as summarized in Table 1. The depression of epoxy cohesive energy under the influence of water is consistent with the experimental observa-

tion on various polymers [48,49]. Meanwhile, the non-bonded interaction energy of epoxy molecule is smaller at elevated temperature in both dry and wet conditions, which is also observed in a simulation study of a similar epoxy material [50]. Furthermore, it is shown in a recent MD simulation study that the glass transition temperature (T_g) of epoxy in the interface changes from 459 K in dry condition to the lower temperature of 382 K in wet condition, as determined by measuring the epoxy molecular mobility at different temperature levels, and the decrease of T_g is correlated to the loss of epoxy cohesive energy as well [29]. As the cohesive energy determines the magnitude of epoxy thermo-mechanical properties [51,52], the reduction of epoxy cohesive energy demonstrates the weakening of epoxy properties due to the detrimental effect of hygrothermal conditioning. During the equilibration process, the epoxy molecule forms a thin and densely packed layer in the vicinity of fiber surface, which possesses decreased number density and more severe energy concentration in hygrothermal condition, and it is associated with the deterioration of the local fiber/matrix interface, as discussed in a recent MD simulation study [29].

3.2. Normal separation of fiber/matrix interface

The interfacial separation simulations described in the previous section are performed to determine the interfacial mechanical properties of fiber/matrix interface under various environmental exposures. The force-displacement curves measured during the normal separation process for dry and wet interfaces are shown in Fig. 4(a). The normal separation force experienced by the epoxy molecule is normalized by the total number of atoms in the epoxy molecule. Regarding the curves, the separation distance of zero corresponds to the equilibrium configuration of the interfaces after the structural equilibration. Three distinguished stages are observed from the curves, which correspond to the separation force-displacement curves from similar epoxy-graphene interfaces [53,54]. The peak force denoting the transition from first to second stage is measured as 2.55 pN in dry condition at $27 \text{ }^\circ\text{C}$, which is comparable to the value of separating different polymers from the planar substrates, in the range of $1.4\text{--}7.2 \text{ pN}$ [54–57]. When water is added, the peak force is reduced by 28.0% and the exposure to the elevated temperature level further decreases the peak force in both conditions, with the largest reduction by 35.3% in the hygrothermal environment. The lower level of peak force suggests a lower interfacial fracture energy. This quantity is defined as the energy required to separate the interface from the equilibrium state to the completely separated state, which is represented by the potential of mean force (PMF) as constructed by integrating the force-displacement curve and summarized in Fig. 4(b). The fracture energy of fiber/matrix interface is calculated as $2811.6 \text{ kcal}\cdot\text{mol}^{-1}$ in $27 \text{ }^\circ\text{C}$ dry condition. According to the interface investigations using MD simulations, it is found that the interfacial fracture energy between different polymers and the graphene sheet ranges from 643 to $16112 \text{ kcal}\cdot\text{mol}^{-1}$ [55,58–60]. The simulated fracture energy of fiber/matrix interface is within the range reported in these different simulation studies. It is learned that the bonding nature of these different systems is similar, which is governed by the vdW interaction, and the variation of the reported interfacial energies can be attributed to the differences in the investigated polymers, model sizes, force fields, and simulation approaches. With the presence of water molecules, the fracture energy of fiber/matrix interface decreases to $1059.6 \text{ kcal}\cdot\text{mol}^{-1}$, which equals to a decrease of nearly 62.3%. Moreover, the most severe degradation is up to 68.7% in the hygrothermal environment. The simulation result demonstrates that the hygrothermal environment severely reduces the peak force and fracture energy

Table 1
Energy of the non-bonded interactions between epoxy atoms averaged from the last 30 ps equilibration.

	Non-bonded interaction energy ($\text{kcal}\cdot\text{mol}^{-1}$)
Dry, $27 \text{ }^\circ\text{C}$	3772.0 ± 6.9
Dry, $50 \text{ }^\circ\text{C}$	3708.5 ± 8.9
Wet, $27 \text{ }^\circ\text{C}$	3048.2 ± 9.7
Wet, $50 \text{ }^\circ\text{C}$	2940.7 ± 18.9

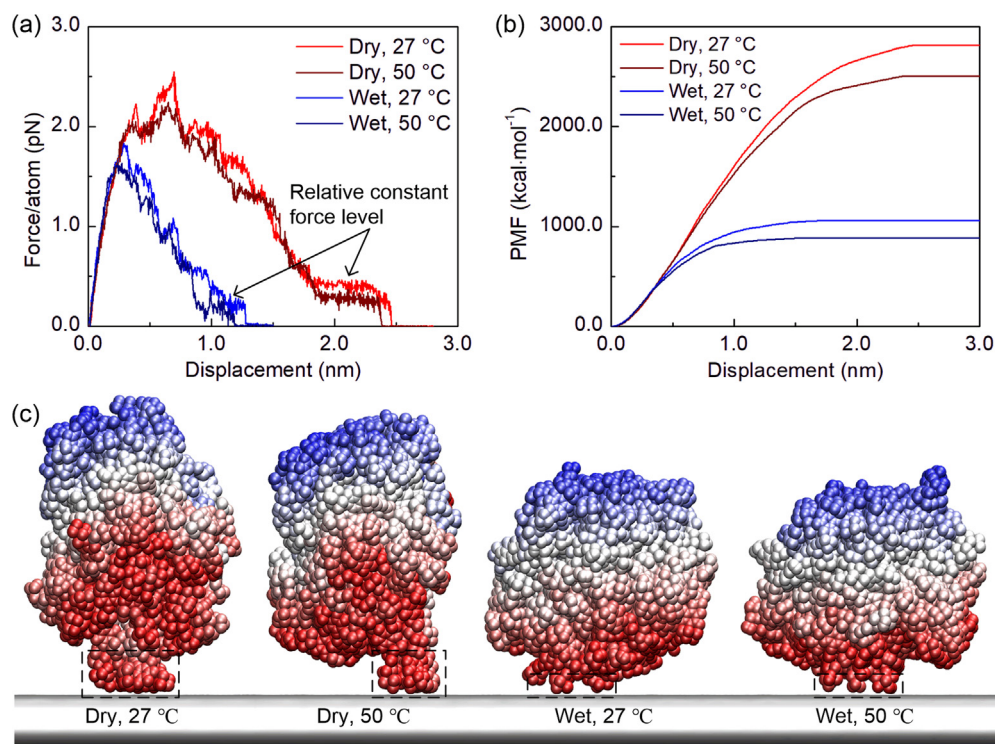


Fig. 4. (a) The force-displacement curves and (b) interfacial fracture energies from normal separation simulations of the interfaces under various environmental exposures: the fracture energy is represented by the potential of mean force (PMF) as constructed by integrating the force-displacement curve. (c) The simulation snapshots from the third stage in force-displacement curves corresponding to the relative constant level of pulling force before final separation: for dry interfaces, there is a residual epoxy structure observed to form a bridge between detached epoxy portion and planar wall, as indicated by the dotted rectangle; for wet interfaces, the bridge is not obvious, which is responsible for the decreased adhesion energy. At elevated temperature of 50 °C, the epoxy becomes softened, which possesses a decreased adhesion to the bonded material as compared to the cases at 27 °C. The atom of epoxy molecule is colored according to its vertical distance from the planar wall before the pulling simulations, and water molecules are not shown for clarity.

necessary to separate the fiber/matrix interface, thereby making such interfaces weaker and degrading the composite properties.

In order to understand why the decreasing trends are observed in the hygrothermal environment, a more detailed examination of the molecular behavior of the interface is necessary. Due to the interaction with water molecules, the epoxy possesses various properties under different environmental exposures, which can affect the interfacial behaviors during the separation simulation. The simulation snapshots from the third stage in force-displacement curves corresponding to the relative constant level of pulling force before final separation are shown in Fig. 4(c), which illustrates key differences in dry and wet conditions. For the dry interfaces at both temperature levels, there is a residual epoxy structure observed to form a bridge between detached epoxy portion and planar wall before final separation. This hair-like bridge has also been observed in the debonding test between epoxy and silica substrate [61]. However, for the wet interfaces, it is observed that during the separation, water molecules tend to diffuse into the available space between debonded portion and substrate. The strong polar interactions between water and epoxy promote the debonding process, which consequently make the hair-like bridge not obvious. In this case, the hair-like bridge formed by the epoxy results in an extension of the interface to fail at approximately 2.4 nm in dry conditions, which decreases to 1.2 nm in wet conditions. This decrease hence leads to the decreased interfacial fracture energy in wet conditions. At elevated temperature of 50 °C, the epoxy transits to a state close to the glass transition and becomes softened, as demonstrate by the decreased cohesive energy of epoxy molecule as shown in Table 1. The softened epoxy possesses a decreased adhesion to the bonded material as compared to the cases at 27 °C.

3.3. Shearing of fiber/matrix interface

Apart from the interfacial separation behavior, the shear behavior of the fiber/matrix interface is of great concern as the interfacial shear properties are strongly influenced when the composite is conditioned in the hygrothermal environment. The shear force-displacement curves measured from the SMD shear simulations for dry and wet interfaces are shown in Fig. 5(a). The shear force increases rapidly during the initial loading process, and then increases slowly as the epoxy starts to slide, and finally plateaus as the epoxy reaches the steady sliding stage. It is noted that during the loading process, the epoxy molecule is sheared along the periodic planar wall, and after reaching the steady sliding stage, the distance between epoxy molecule and planar wall remains fairly constant, and the vdW interactions between two materials exist continuously. Therefore, the force plateaus during the steady sliding stage and the final drop in the shear force corresponding to the interfacial failure is not captured. In order to represent the fully detached state, the derived traction-separation curves can be cut-off where the epoxy reaches the steady sliding stage, and the final drop in the shear force corresponding to the interfacial failure can be included. Although the final interfacial detachment is not observed here, the derived force-displacement curves correspond closely to those obtained from the shear simulation of bilayer interfaces between epoxy and graphene sheets as well as between iron and precipitate [53,54,62], and also show a close correlation with the detachment initiation and propagation in the load-displacement curve from single-fiber pullout test and finite element simulation [63]. When compared to the peak force of normal separation simulation, it is observed that the level of shear force plateau for all the simulated conditions is comparatively lower,

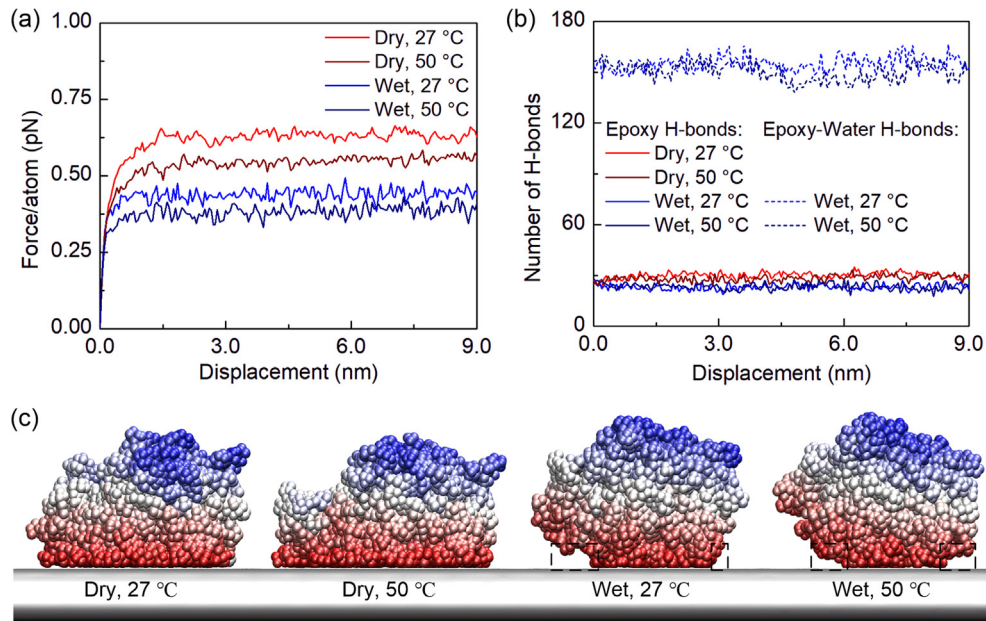


Fig. 5. (a) The force-displacement curves from shear simulations of the interfaces under various environmental exposures: water effectively reduces the sliding friction between fiber and matrix. (b) This decrease can be attributed to a disruption of epoxy-epoxy hydrogen bonds (H-bonds), which are disrupted or replaced by epoxy-water hydrogen bonds in wet conditions, and (c) the epoxy molecule transits from the closely attached state in dry conditions to the slightly detached state in wet conditions, as indicated by the dotted rectangle. The simulation snapshots are from the level of force plateau close to the end of shear simulation. Color codes are the same as in Fig. 4.

which is consistent with the simulation results of similar epoxy-bonded interfaces [53,54]. The lower level of shear force as compared to the separation force suggests the lower resistance of the fiber/matrix interface to the shear load. In dry condition at 27 °C, the level of shear force plateau is measured as 0.63 ± 0.01 pN, which is in a close agreement with the results obtained from shearing different polymers from the planar substrate, with the value of 0.4–2.0 pN [55–57]. In the presence of water molecules, the level of shear force plateau shows similar trends to the normal separation simulation, where the exposure to the wet environment at 27 and 50 °C leads to the reduction by 30.3% and 38.2% respectively, as compared to the dry case at 27 °C. The detrimental effect of wet and hygrothermal condition on the interfacial shear properties of carbon fiber/epoxy interface has also been observed in the micro-bond test [10,27,64,65]. Specifically, the interfacial shear strength of fiber/matrix interface decreases by 9% and 33% after room-temperature water immersion for 20 days [10] and for 30 days [27] respectively, and by 41% after conditioning at 95% relative humidity at 40 °C for 24 days [64] and also after 80 °C water immersion for 6 h [65] respectively. Meanwhile, a more severe deterioration in the interfacial shear properties of fiber/matrix interface is observed with the increasing conditioning temperature in the wet environment [66]. Although there is not a general agreement over the degree of degradation, the observed reduction of shear force by 30.3% and 38.2% in water at 27 and 50 °C is within the range reported in the experimental studies, and the decreasing trend of interfacial shear properties at elevated temperatures agrees with the experimental observation as well. The simulation result demonstrates that water molecules effectively reduce the energy barrier to induce shearing between fiber and matrix.

The decreasing trend in shear force can be explained by the disruption of fiber/matrix interaction due to the presence of water molecules. During the shear deformation, the epoxy molecule interacts with the planar wall through the non-bonded interaction represented by a vdW potential term. As seen in Fig. 5(c), the epoxy attaches closely to the bonded wall in dry condition at both temperature levels. The simulation snapshots are from the level of force plateau close to the end of shear simulation. When the inter-

face is conditioned in the wet environment, the functional groups of epoxy molecule interact favorably with water molecules [67]. As shown in Fig. 5(b), the number of hydrogen bond (which is calculated using distance cutoff of 0.35 nm and angle cutoff of 130 °C [68]) between epoxy functional groups decreases slightly in the wet environment. This decrease can be directly attributed to the interaction of epoxy molecule being disrupted or replaced by the epoxy-water hydrogen bonds, as shown in Fig. 5(b). The favorable epoxy-water interaction leads to a slight detachment of epoxy molecule and the degradation of epoxy properties, as is also discussed in the previous section. During the shear simulation, the water molecules tend to fill into the empty space between the bonded materials, as similar to the wet cases in normal separation simulation. Therefore, due to the polar interactions with the water molecules, the bonded materials possess reduced contact area and the epoxy properties degrade, and hence the interface exhibits decreased resistance to the shear deformation.

3.4. Discussion of fiber/matrix interfacial response in hygrothermal environment

The simulation results of structural equilibration and traction-separation simulation have been presented for fiber/matrix interfaces in order to study the effects of the hygrothermal environment on interfacial integrity. Both the separation and shear simulations reveal that the water molecules decrease the energy required to separate or shear the epoxy molecule from the bonded surface, and the reduction is more severe at the elevated temperature level. Our results suggest that in dry condition, there is a close contact between fiber and matrix, ensuring the strong interfacial integrity of the CFRP composite in various applications. However, due to the polar interactions between epoxy and water, the matrix could detach slightly; meanwhile, water molecules entering the empty space in the detached area could accelerate the epoxy detachment, making the interface vulnerable to the hygrothermal environment. The results from the traction-separation simulations of fiber/matrix interface can be used to derive the cohesive law, which can be implemented in a larger-scale simulation for investigating the

composite, with the consideration of the environmental effects on the traction-separation relations of fiber/matrix interface. A brief discussion about the development of cohesive laws for fiber/matrix interface is included in the [Appendix C](#).

As the simulations here are conducted using ideal planar wall to represent the fiber surface without considering the surface treatments, the computed absolute value of the simulation results may not exactly match the experimental data, while the computed values are still comparable with various MD simulation results from the interfacial separation and shearing tests on different polymer-graphene interfaces [53–60,62]. Meanwhile, it is noted that the variation of interfacial mechanical properties as observed here represents the most valuable information for understanding the interfacial deterioration mechanism in the hygrothermal environment, as the observed variation enables one to focus on the most critical factors that affect the integrity of fiber/matrix interface. Due to the advance in chemistry, it allows for more complex, tailored modifications of fiber surface. The molecular model developed in this work can be adapted to simulate the functionalized graphene sheets to represent the treated fiber surface, and the simulation strategy used here can be applicable to investigating the traction-separation behavior of the fiber/matrix interface with various surface characteristics, so as to develop the fiber/matrix interface with improved resistance to the hygrothermal environment.

4. Conclusions

In this study, atomistic SMD simulations are employed to investigate the traction-separation response of fiber/matrix interface in the hygrothermal environment. The molecular model of fiber/matrix interface is conditioned in a water box at the elevated temperature level to simulate the hygrothermal environment. In dry condition, the interface possesses stronger resistance to the interfacial separation and shear, as epoxy molecule attaches closely to the bonded surface and can form the hair-like bridge that increases the extension before final separation. In the presence of water, the interface exhibits decreased adhesion and shear resistance as the epoxy-water polar interaction results in the slight detachment of epoxy molecule, which leads to the accumulation of water molecules in the detached area close to the interface and thereby degrades interfacial mechanical properties. The degradation of interfacial traction-separation response is more severe at elevated temperature, as the epoxy molecule becomes softened at the state close to glass transition, and detaches/slides from the bonded surface more easily under the external load. The traction-separation responses are used to develop the cohesive zone model, which will help model the fiber/matrix interfacial fracture in composites in a large-scale simulation. These results are an important first step towards the investigation of environment-affected interfacial integrity in FRP composites. While we have specifically used the planar wall to represent the clean surface of fiber, the computational approach can be easily adapted to rapidly evaluate the fiber surface morphologies with different chemical modifications to assess the water tolerance of the interfacial mechanical properties. These techniques not only provide atomistic insights into the interfacial properties of fiber/matrix interface under the environmental exposure, but also provide the paradigm for deriving the fundamental inputs for a multiscale analysis about how the environment-affected interfacial bonding can affect the macroscale composite properties.

Declaration of Competing Interest

None.

Acknowledgements

This work was supported by the National Natural Science Foundation of China (Grant No. 51608020, 51808020) and by the China Postdoctoral Science Foundation (Grant No. 2017M620015, 2018T110029). The support from the Thousand Talents Plan (Young Professionals) in China was also gratefully acknowledged.

Appendix A. Details of molecular interface model

In this study, epoxy monomers are connected by the covalent bond to achieve the cross-link in the structure [29,33,36]. The epoxy monomer consists of four bisphenol A diglycidyl ethers (DGEBA) connected by the methylene group, which is consistent with the SU-8 monomer [33,36]. DGEBA is the basic component of epoxy resin used in CFRP fabrication, and the epoxy molecule cross-linked from the monomer formed by DGEBA possesses the common structural characteristics of epoxy resin, including high cross-linking degree [28], which is an important analogue of the epoxy models with various cross-linking agents. The epoxy molecule interacts with the planar wall representing the fiber out-layer through the non-bonded vdW interaction, which is calculated by a 12–6 Lennard-Jones (LJ) potential, and it is a generally used term for the vdW interaction between the bonded materials:

$$E_{\text{LJ}}(r) = 4\varepsilon_{\text{LJ}} \left[\left(\frac{\sigma_{\text{LJ}}}{r} \right)^{12} - \left(\frac{\sigma_{\text{LJ}}}{r} \right)^6 \right] \quad r \leq r_{\text{cut}}, \quad (\text{A.1})$$

where σ_{LJ} and ε_{LJ} are the two potential energy parameters denoting the distance at which E_{LJ} is zero and the interaction strength respectively, and r_{cut} is the cutoff distance of interaction with a value of 1.0 nm, same as that defined for the vdW interaction in the system. The value of $\sigma_{\text{LJ}} = 0.4$ nm and $\varepsilon_{\text{LJ}} = 3.0$ kcal·mol⁻¹ are chosen to lead to a surface energy of around 100.0 mJ·m⁻² for the planar wall, which is comparable with that of graphite or graphene sheets between 50 and 175 mJ·m⁻² [69–72]. Therefore, it is expected that the structural behavior of the fiber/matrix interface can be interpreted by investigating the interface formed by the DGEBA-based epoxy and the ideal planar energetic wall in this study.

Appendix B. Dependence of pulling rate on interfacial mechanics

In steered molecular dynamics (SMD) simulation, the dependence of pulling rate on probing the nanoscale mechanics is a typical concern. To show that the force-displacement curve obtained from the selected rate of 2.5 m·s⁻¹ does not exhibit significant rate dependence, a set of interfacial separation simulations are carried out by varying the rate from 0.5 to 100 m·s⁻¹. The force-displacement curves obtained from separating the dry interface at the temperature level of 27 °C are shown in [Fig. B.1](#). At high pulling rates over 10 m·s⁻¹, the peak separation force increases with the increasing pulling rate, and the curves show slight differences in shape. At pulling rates ranging from 0.5 to 5 m·s⁻¹, the force-displacement curves do not change significantly. To capture the proper interfacial failure mechanism and also consider the computational cost, a sufficiently slow rate of 2.5 m·s⁻¹ is selected in the simulations.

For the rate dependence on the interfacial shear behavior, a recent study on the interfacial mechanics of cellulose nanocrystals has shown that the shear force-displacement curves do not change significantly for pulling rate ranging from 0.5 to 5 m·s⁻¹ [73]. Given that the bonding nature of fiber/matrix interface and cellulose nanocrystals interface is similar, which is dominated by the non-bonded interaction, it is inferred that the shear force-displacement curves of fiber/matrix interface would not change

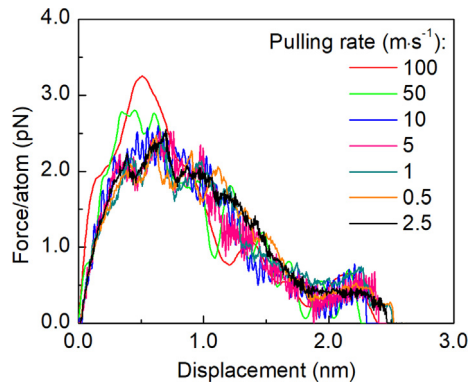


Fig. B.1. The force-displacement curves from separating the dry interface at the temperature level of 27 °C with different pulling rates. A pulling rate of 2.5 m·s⁻¹ is selected for the simulations in which the traction-separation behavior is determined.

significantly at the same slow deformation regime. Meanwhile, the pulling rate of 2.5 m·s⁻¹ has been successfully used in the simulation of the interfacial shear behavior between different polymers and planar substrates in previous studies [54–57]. Therefore, it is believed that the pulling rate of 2.5 m·s⁻¹ is applicable to the shear simulations of fiber/matrix interface in this study.

Appendix C. Development of cohesive laws for fiber/matrix interface

The data from the traction-separation simulations of fiber/matrix interface is used to define the cohesive law, which can be integrated into a continuum model for the interface to be used in a multiscale analysis. Based on the results of interfacial separation simulations for both the dry and wet interfaces, the cohesive formulation is developed to represent the traction-separation response under normal separation loading. Although the interfaces in dry and wet conditions exhibit different debonding processes, notably the different formations of hair-like bridge before final separation, the force-displacement curves shown in Fig. 4(a) indi-

cate that the evolution of normal separation force during the pulling process is similar. This similarity suggests that the interfacial separation for the interfaces can be described using the same analytical formulation. Based on the normal separation force-displacement curves, the mode I traction-separation response is derived from normalizing the total force on epoxy molecule by the contact area, as shown in Fig. C.1(a). The derived interfacial mode I traction-separation response has the exponential form and is fitted by the exponential cohesive zone model [57,58,74]:

$$T_1 = T_{1c} \left(\frac{u_1}{u_{1c}} \right) \exp \left(1 - \frac{u_1}{u_{1c}} \right), \quad (\text{C.1})$$

where T_{1c} is the peak traction and u_{1c} is the separation displacement at $T_1 = T_{1c}$. The fitted curves for the separation response are shown in Fig. C.1(a), with the calculated coefficients of determination all over 95.8%. According to the fitted curves, the peak normal traction and separation displacement at peak traction are determined and summarized in Table C.1. In dry condition at 27 °C, the peak traction of 254.40 MPa and the corresponding displacement of 0.532 nm are consistent with the MD-based cohesive zone model parameters of different polymer-graphene interfaces ranging from 171 to 450 MPa and 0.2 to 0.5 nm, respectively [54–56,58]. Meanwhile, the work of separation is calculated by integrating the fitted curves with respect to the separation displacement. Notably, the work of separation in dry condition at 27 °C is measured as 367.70 mJ·m⁻², which agrees closely with the value for the interfaces between different polymers and graphene sheets ranging from 129.1 to 560.3 mJ·m⁻² [54–56,58]. It suggests that the investigated interface model here is able to represent the nature of the interfacial bonding between fiber and matrix. By comparing the peak normal traction and work of separation in different conditions, it is confirmed that the hygrothermal environment is detrimental to the interfacial integrity between fiber and matrix.

In addition to the separation simulation, the cohesive formulation is developed to represent the interfacial response under shear loading. Although the epoxy molecule in wet conditions exhibit a slight detachment due to the favorable interaction with water, the overall shape and behavior in terms of traction response as shown in Fig. 5(a) is similar for both dry and wet interfaces. This

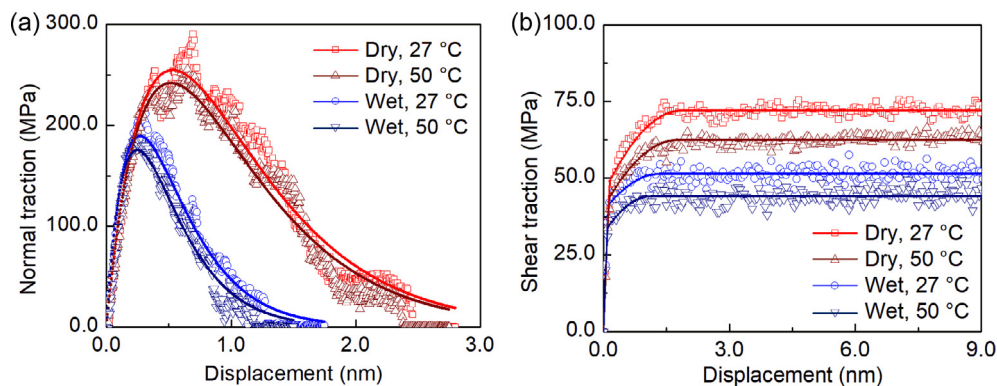


Fig. C.1. The (a) mode I and (b) mode II cohesive zone laws (solid lines) for the molecular fiber/matrix interface derived from the traction-separation responses (scattered points) from MD simulations under various environmental exposures.

Table C.1

Cohesive zone model parameters for normal separation of fiber/matrix interface under various environmental exposures.

	Peak normal traction (MPa)	Separation displacement at peak traction (nm)	Work of separation (mJ·m ⁻²)
Dry, 27 °C	254.40	0.532	367.70
Dry, 50 °C	241.63	0.518	340.39
Wet, 27 °C	189.10	0.271	139.13
Wet, 50 °C	175.35	0.248	118.05

Table C.2

Cohesive zone model parameters for the shearing of fiber/matrix interface under various environmental exposures.

	Shear displacement and traction where epoxy starts to slide		Shear displacement and traction where epoxy reaches steady sliding stage	
	Shear displacement (nm)	Shear traction (MPa)	Shear displacement (nm)	Shear traction (MPa)
Dry, 27 °C	0.133	44.64	1.877	72.02
Dry, 50 °C	0.127	43.37	1.771	62.37
Wet, 27 °C	0.109	41.10	1.361	51.37
Wet, 50 °C	0.084	33.56	1.137	44.04

enables the use of the same analytical formulation to describe the shear response of fiber/matrix interface under different environmental exposures. Accordingly, the mode II traction-separation response during the interfacial shear simulation can be approximated by the cohesive zone model with three parts [62]:

$$T_{II} = \begin{cases} \frac{T_{IIc1}}{u_{IIc1}} u_{II}, & u_{II} \leq u_{IIc1} \\ \frac{T_{IIc1} - T_{IIc2}}{(u_{IIc1} - u_{IIc2})^2} (u_{II} - u_{IIc1})^2 + T_{IIc2}, & u_{IIc1} \leq u_{II} \leq u_{IIc2} \\ T_{IIc2}, & u_{II} \geq u_{IIc2} \end{cases} \quad (C.2)$$

where u_{IIc1} is the shear displacement when the epoxy starts to slide, T_{IIc1} is the corresponding value of shear traction, u_{IIc2} is the shear displacement when the epoxy reaches the steady sliding stage, and T_{IIc2} is the corresponding shear traction. The fitted curves for the interfacial shear response in different conditions are shown in Fig. C.1(b), with the calculated coefficients of determination all over 76.6%. As discussed previously, the shear simulation is performed along the periodic planar wall, and thus the drop in shear traction corresponding to total interfacial failure is not captured by these equations. The parameters for the cohesive law are summarized in Table C.2 for all the interfaces. For the dry interface at 27 °C, the shear traction where the epoxy reaches the steady sliding stage is calculated as 72.02 MPa, which is close to the cohesive zone model parameter for the similar polymer-graphene interfaces, with the value of 50–80 MPa [54,56]. By comparing the level of shear displacement and traction in different conditions, it further confirms the detrimental effect of the hygrothermal environment on the fiber/matrix interface.

References

- [1] L. Van Den Einde, L. Zhao, F. Seible, Use of FRP composites in civil structural applications, *Constr. Build. Mater.* 17 (6) (2003) 389–403.
- [2] X. Zheng, P. Huang, G. Chen, X.M. Tan, Fatigue behavior of FRP-concrete bond under hygrothermal environment, *Constr. Build. Mater.* 95 (2015) 898–909.
- [3] Z. Wang, X.-L. Zhao, G. Xian, G. Wu, R.K. Singh Raman, S. Al-Saadi, Durability study on interlaminar shear behaviour of basalt-, glass- and carbon-fibre reinforced polymer (B/G/CFRP) bars in seawater sea sand concrete environment, *Constr. Build. Mater.* 156 (2017) 985–1004.
- [4] L.C. Hollaway, A review of the present and future utilisation of FRP composites in the civil infrastructure with reference to their important in-service properties, *Constr. Build. Mater.* 24 (12) (2010) 2419–2445.
- [5] D. Lau, Q. Qiu, A. Zhou, C.L. Chow, Long term performance and fire safety aspect of FRP composites used in building structures, *Constr. Build. Mater.* 126 (2016) 573–585.
- [6] J.J. Imaz, J.L. Rodriguez, A. Rubio, I. Mondragon, Hydrothermal environment influence on water diffusion and mechanical behaviour of carbon fibre/epoxy laminates, *J. Mater. Sci. Lett.* 10 (11) (1991) 662–665.
- [7] A. Zafar, F. Bertocco, J. Schjødt-Thomsen, J.C. Rauhe, Investigation of the long term effects of moisture on carbon fibre and epoxy matrix composites, *Compos. Sci. Technol.* 72 (6) (2012) 656–666.
- [8] J.H.S. Almeida, S.D.B. Souza, E.C. Botelho, S.C. Amico, Carbon fiber-reinforced epoxy filament-wound composite laminates exposed to hygrothermal conditioning, *J. Mater. Sci.* 51 (9) (2016) 4697–4708.
- [9] Z. Wang, G. Xian, X.-L. Zhao, Effects of hydrothermal aging on carbon fibre/epoxy composites with different interfacial bonding strength, *Constr. Build. Mater.* 161 (2018) 634–648.
- [10] B. Yu, Z. Jiang, J. Yang, Long-term moisture effects on the interfacial shear strength between surface treated carbon fiber and epoxy matrix, *Compos. Part A Appl. S.* 78 (2015) 311–317.
- [11] J. Zhou, J.P. Lucas, Hygrothermal effects of epoxy resin. Part I: the nature of water in epoxy, *Polymer* 40 (20) (1999) 5505–5512.
- [12] J.N. Myers, C. Zhang, K.-W. Lee, J. Williamson, Z. Chen, Hygrothermal aging effects on buried molecular structures at epoxy interfaces, *Langmuir* 30 (1) (2014) 165–171.
- [13] M.A. Abanilla, Y. Li, V.M. Karbhari, Durability characterization of wet layup graphite/epoxy composites used in external strengthening, *Compos. Part B Eng.* 37 (2–3) (2006) 200–212.
- [14] Y. Gu, H. Liu, M. Li, Y. Li, Z. Zhang, Macro- and micro-interfacial properties of carbon fiber reinforced epoxy resin composite under hygrothermal treatments, *J. Reinf. Plast. Compos.* 33 (4) (2014) 369–379.
- [15] Y. Wang, T.H. Hahn, AFM characterization of the interfacial properties of carbon fiber reinforced polymer composites subjected to hygrothermal treatments, *Compos. Sci. Technol.* 67 (1) (2007) 92–101.
- [16] Y. Gu, M. Li, J. Wang, Z. Zhang, Characterization of the interphase in carbon fiber/polymer composites using a nanoscale dynamic mechanical imaging technique, *Carbon* 48 (11) (2010) 3229–3235.
- [17] Y.-F. Niu, Y. Yang, X.-R. Wang, Investigation of the interphase structures and properties of carbon fiber reinforced polymer composites exposed to hydrothermal treatments using peak force quantitative nanomechanics technique, *Polym. Compos.* 39 (S2) (2018) E791–E796.
- [18] P.-S. Shin, J.-H. Kim, H.-S. Park, Y.-M. Baek, D.-J. Kwon, K.L. DeVries, J.-M. Park, Evaluation of thermally-aged carbon fiber/epoxy composites using acoustic emission, electrical resistance and thermogram, *Compos. Struct.* 196 (2018) 21–29.
- [19] F. Naya, C. González, C.S. Lopes, S. Van der Veen, F. Pons, Computational micromechanics of the transverse and shear behavior of unidirectional fiber reinforced polymers including environmental effects, *Compos. Part A Appl. S.* 92 (2017) 146–157.
- [20] F. Naya, M. Herráez, C.S. Lopes, C. González, S. Van der Veen, F. Pons, Computational micromechanics of fiber kinking in unidirectional FRP under different environmental conditions, *Compos. Sci. Technol.* 144 (2017) 26–35.
- [21] F. Naya, J.M. Molina-Aldareguía, C.S. Lopes, C. González, J. Llorca, Interface characterization in fiber-reinforced polymer-matrix composites, *JOM* 69 (1) (2017) 13–21.
- [22] S. González, G. Laera, S. Koussios, J. Domínguez, F.A. Lasagni, Simulation of thermal cycle aging process on fiber-reinforced polymers by extended finite element method, *J. Compos. Mater.* 52 (14) (2018) 1947–1958.
- [23] P.F. Liu, X.K. Li, A large-scale finite element model on micromechanical damage and failure of carbon fiber/epoxy composites including thermal residual stress, *Appl. Compos. Mater.* 25 (3) (2018) 545–560.
- [24] H. Wang, X. Zhang, Y. Duan, L. Meng, Experimental and numerical study of the interfacial shear strength in carbon fiber/epoxy resin composite under thermal loads, *Int. J. Polym. Sci.* 2018 (2018) 8.
- [25] C. Li, A.R. Browning, S. Christensen, A. Strachan, Atomistic simulations on multilayer graphene reinforced epoxy composites, *Compos. Part A Appl. S.* 43 (8) (2012) 1293–1300.
- [26] C.M. Hadden, B.D. Jensen, A. Bandyopadhyay, G.M. Odegard, A. Koo, R. Liang, Molecular modeling of EPON-862/graphite composites: interfacial characteristics for multiple crosslink densities, *Compos. Sci. Technol.* 76 (2013) 92–99.
- [27] Y. Xiao, G. Xian, Effects of moisture ingress on the bond between carbon fiber and epoxy resin investigated with molecular dynamics simulation, *Polym. Compos.* 39 (S4) (2018) E2074–E2083.
- [28] L.-h. Tam, L. He, C. Wu, Molecular dynamics study on the effect of salt environment on interfacial structure, stress, and adhesion of carbon fiber/epoxy interface, *Compos. Interfaces* 26 (5) (2019) 431–447.
- [29] L.-h. Tam, A. Zhou, C. Wu, Nanomechanical behavior of carbon fiber/epoxy interface in hygrothermal conditioning: a molecular dynamics study, *Mater. Today Commun.* (2019) 495–505.
- [30] D. Hou, T. Zhao, H. Ma, Z. Li, Reactive molecular simulation on water confined in the nanopores of the calcium silicate hydrate gel: structure, reactivity, and mechanical properties, *J. Phys. Chem. C* 119 (3) (2015) 1346–1358.
- [31] D. Hou, Z. Lu, X. Li, H. Ma, Z. Li, Reactive molecular dynamics and experimental study of graphene-cement composites: structure, dynamics and reinforcement mechanisms, *Carbon* 115 (2017) 188–208.
- [32] N. Tual, N. Carrere, P. Davies, T. Bonnemaïn, E. Lolive, Characterization of sea water ageing effects on mechanical properties of carbon/epoxy composites for tidal turbine blades, *Compos. Part A Appl. S.* 78 (2015) 380–389.
- [33] L.-h. Tam, D. Lau, A molecular dynamics investigation on the cross-linking and physical properties of epoxy-based materials, *RSC Adv.* 4 (62) (2014) 33074–33081.
- [34] R.W. Hockney, J.W. Eastwood, *Computer Simulation using Particles*, CRC Press, Boca Raton, 1988.

- [35] T. Oie, G.M. Maggiora, R.E. Christoffersen, D.J. Duchamp, Development of a flexible intra- and intermolecular empirical potential function for large molecular systems, *Int. J. Quantum Chem.* 20 (58) (1981) 1–47.
- [36] L.-h. Tam, D. Lau, Moisture effect on the mechanical and interfacial properties of epoxy-bonded material system: an atomistic and experimental investigation, *Polymer* 57 (2015) 132–142.
- [37] L.-h. Tam, C.L. Chow, D. Lau, Moisture effect on interfacial integrity of epoxy-bonded system: a hierarchical approach, *Nanotechnology* 29 (2) (2018) 024001.
- [38] C. Wu, R. Wu, L.-h. Tam, Atomistic investigation on interfacial deterioration of epoxy-bonded interface under hygrothermal environment, 9th International Conference on Fibre-Reinforced Polymer (FRP) Composites in Civil Engineering (CICE 2018), 2018.
- [39] W.L. Jorgensen, J. Chandrasekhar, J.D. Madura, R.W. Impey, M.L. Klein, Comparison of simple potential functions for simulating liquid water, *J. Chem. Phys.* 79 (2) (1983) 926–935.
- [40] S. Plimpton, Fast parallel algorithms for short-range molecular dynamics, *J. Comput. Phys.* 117 (1) (1995) 1–19.
- [41] S. Nouranian, C. Jang, T.E. Lacy, S.R. Gwaltney, H. Toghiani, C.U. Pittman, Molecular dynamics simulations of vinyl ester resin monomer interactions with a pristine vapor-grown carbon nanofiber and their implications for composite interphase formation, *Carbon* 49 (10) (2011) 3219–3232.
- [42] C. Jang, T.E. Lacy, S.R. Gwaltney, H. Toghiani, C.U. Pittman, Interfacial shear strength of cured vinyl ester resin-graphite nanoplatelet from molecular dynamics simulations, *Polymer* 54 (13) (2013) 3282–3289.
- [43] W. Shinoda, M. Shiga, M. Mikami, Rapid estimation of elastic constants by molecular dynamics simulation under constant stress, *Phys. Rev. B* 69 (13) (2004) 134103.
- [44] G.C. Mays, A.R. Hutchinson, *Adhesives in Civil Engineering*, Cambridge University Press, Cambridge, 2005.
- [45] A. Einstein, *Investigations on the Theory of the Brownian Movement*, Courier Dover Publications, New York, 1956.
- [46] R. Mills, Self-diffusion in normal and heavy water in the range 1–45. deg, *J. Phys. Chem.* 77 (5) (1973) 685–688.
- [47] A. Zhou, L.-h. Tam, Z. Yu, D. Lau, Effect of moisture on the mechanical properties of CFRP-wood composite: an experimental and atomistic investigation, *Compos. Part B Eng.* 71 (2015) 63–73.
- [48] H. Batzer, U.T. Kreibich, Influence of water on thermal transitions in natural polymers and synthetic polyamides, *Polym. Bull.* 5 (11) (1981) 585–590.
- [49] A. Blanchard, F. Gouanvé, E. Espuche, Effect of humidity on mechanical, thermal and barrier properties of EVOH films, *J. Membr. Sci.* 540 (2017) 1–9.
- [50] C. Li, A. Strachan, Cohesive energy density and solubility parameter evolution during the curing of thermoset, *Polymer* 135 (2018) 162–170.
- [51] M.J. Marks, R.V. Snelgrove, Effect of conversion on the structure–property relationships of amine-cured epoxy thermosets, *ACS Appl. Mater. Interfaces* 1 (4) (2009) 921–926.
- [52] W. Zhang, Y. Qing, W. Zhong, G. Sui, X. Yang, Mechanism of modulus improvement for epoxy resin matrices: a molecular dynamics simulation, *React. Funct. Polym.* 111 (2017) 60–67.
- [53] N. Subramanian, A. Rai, A. Chattopadhyay, Atomistically derived cohesive behavior of interphases in carbon fiber reinforced CNT nanocomposites, *Carbon* 117 (2017) 55–64.
- [54] Y. Li, G.D. Seidel, Multiscale modeling of the interface effects in CNT-epoxy nanocomposites, *Comput. Mater. Sci.* 153 (2018) 363–381.
- [55] P.A. Amnaya, C.L. Dimitris, C.H. Daniel, Modeling of graphene–polymer interfacial mechanical behavior using molecular dynamics, *Model. Simul. Mater. Sc.* 17 (1) (2009) 015002.
- [56] Y. Li, G.D. Seidel, Multiscale modeling of the effects of nanoscale load transfer on the effective elastic properties of unfunctionalized carbon nanotube–polyethylene nanocomposites, *Model. Simul. Mater. Sc.* 22 (2) (2014) 025023.
- [57] B. Paliwal, W.B. Lawrimore, M.Q. Chandler, M.F. Horstemeyer, Nanomechanical modeling of interfaces of polyvinyl alcohol (PVA)/clay nanocomposite, *Philos. Mag.* 97 (15) (2017) 1179–1208.
- [58] S. Lee, J. Park, J. Yang, W. Lu, Molecular dynamics simulations of the traction-separation response at the interface between PVDF binder and graphite in the electrode of Li-ion batteries, *J. Electrochem. Soc.* 161 (9) (2014) A1218–A1223.
- [59] S.P. Ju, C.C. Chen, T.J. Huang, C.H. Liao, H.L. Chen, Y.C. Chuang, Y.C. Wu, H.T. Chen, Investigation of the structural and mechanical properties of polypropylene-based carbon fiber nanocomposites by experimental measurement and molecular dynamics simulation, *Comput. Mater. Sci.* 115 (2016) 1–10.
- [60] S.J. Nikkha, M.R. Moghbeli, S.M. Hashemianzadeh, Dynamic study of deformation and adhesion of an amorphous polyethylene/graphene interface: a simulation study, *Macromol. Theory Simul.* 25 (6) (2016) 533–549.
- [61] D. Lau, K. Broderick, M.J. Buehler, O. Büyüköztürk, A robust nanoscale experimental quantification of fracture energy in a bilayer material system, *Proc. Natl. Acad. Sci. U.S.A.* 111 (33) (2014) 11990–11995.
- [62] A. Elzas, T.P.C. Klaver, B.J. Thijssse, Cohesive laws for shearing of iron/precipitate interfaces, *Comput. Mater. Sci.* 152 (2018) 417–429.
- [63] J.H. Tsai, A. Patra, R. Wetherhold, Finite element simulation of shaped ductile fiber pullout using a mixed cohesive zone/friction interface model, *Compos. Part A Appl. S.* 36 (6) (2005) 827–838.
- [64] Z. Wang, X. Huang, G. Xian, H. Li, Effects of surface treatment of carbon fiber: tensile property, surface characteristics, and bonding to epoxy, *Polym. Compos.* 37 (10) (2016) 2921–2932.
- [65] D.A. Biro, G. Pleizier, Y. Deslandes, Application of the microbond technique: effects of hygrothermal exposure on carbon-fiber/epoxy interfaces, *Compos. Sci. Technol.* 46 (3) (1993) 293–301.
- [66] P. Sun, Y. Zhao, Y. Luo, L. Sun, Effect of temperature and cyclic hygrothermal aging on the interlaminar shear strength of carbon fiber/bismaleimide (BMI) composite, *Mater. Des.* 32 (8) (2011) 4341–4347.
- [67] L.-h. Tam, D. Lau, C. Wu, Understanding interaction and dynamics of water molecules in the epoxy via molecular dynamics simulation, *Mol. Simul.* 45 (2) (2019) 120–128.
- [68] S. Goudeau, M. Charlot, C. Vergelati, F. Müller-Plathe, Atomistic simulation of the water influence on the local structure of polyamide 6, 6, *Macromolecules* 37 (21) (2004) 8072–8081.
- [69] Y. Hernandez, V. Nicolosi, M. Lotya, F.M. Blighe, Z. Sun, S. De, I.T. McGovern, B. Holland, M. Byrne, Y.K. Gun'ko, J.J. Boland, P. Niraj, G. Duesberg, S. Krishnamurthy, R. Goodhue, J. Hutchison, V. Scardaci, A.C. Ferrari, J.N. Coleman, High-yield production of graphene by liquid-phase exfoliation of graphite, *Nat. Nanotechnol.* 3 (2008) 563–568.
- [70] A. Kozbial, Z. Li, C. Conaway, R. McGinley, S. Dhir, V. Vahdat, F. Zhou, B. D'Urso, H. Liu, L. Li, Study on the surface energy of graphene by contact angle measurements, *Langmuir* 30 (28) (2014) 8598–8606.
- [71] J.-F. Dai, G.-J. Wang, C.-K. Wu, Investigation of the surface properties of graphene oxide and graphene by inverse gas chromatography, *Chromatographia* 77 (3) (2014) 299–307.
- [72] A. Ferguson, I.T. Caffrey, C. Backes, J.N. Coleman, S.D. Bergin, Differentiating defect and basal plane contributions to the surface energy of graphite using inverse gas chromatography, *Chem. Mater.* 28 (17) (2016) 6355–6366.
- [73] Z. Wei, R. Sinko, S. Keten, E. Luijten, Effect of surface modification on water adsorption and interfacial mechanics of cellulose nanocrystals, *ACS Appl. Mater. Interfaces* 10 (9) (2018) 8349–8358.
- [74] G. Xu, H. Wang, Molecular dynamics study of interfacial mechanical behavior between asphalt binder and mineral aggregate, *Constr. Build. Mater.* 121 (2016) 246–254.